PII S0360-3016(02)02811-0

PHYSICS CONTRIBUTION

ELECTRON CONFORMAL RADIOTHERAPY USING BOLUS AND INTENSITY MODULATION

Rajat J. Kudchadker, Ph.D.,* Kenneth R. Hogstrom, Ph.D.,* Adam S. Garden, M.D.,[†]
Marsha D. McNeese, M.D.,[†] Robert A. Boyd, Ph.D.,* and John A. Antolak, Ph.D.*

Departments of *Radiation Physics and [†]Radiation Oncology, The University of Texas M. D. Anderson Cancer Center, Houston, TX

Purpose: Conformal electron beam therapy can be delivered using shaped bolus, which varies the penetration of the electrons across the incident beam so that the 90% isodose surface conforms to the distal surface of the planning target volume (PTV). Previous use of this modality has shown that the irregular proximal surface of the bolus causes the dose heterogeneity in the PTV to increase from 10%, the typical dose spread of a flat-water surface to approximately 20%. The present work evaluates the ability to restore dose homogeneity by varying the incident electron intensity.
Methods and Materials: Three patients, one each with chest wall, thorax, and head-and-neck cancer, were planned using electron conformal therapy with bolus, with and without intensity modulation. Resulting dose distributions and dose–volume histograms were compared with non-intensity-modulated bolus plans.
Results: In all cases, the $\Delta D_{90\%-10\%}$ for the PTV was reduced; for example, for the head-and-neck case, the $\overline{\Delta D}_{90\%-10\%}$ for the PTV was reduced from 14.9% to 9.2%. This reduction in dose spread is a direct result of intensity modulation.
Conclusions: The results showed that intensity-modulated electron beams could significantly improve the dose homogeneity in the PTV for patients treated with electron conformal therapy using shaped bolus. © 2002 Elsevier Science Inc.

Electron conformal therapy, Electron bolus, Intensity modulation.

INTRODUCTION

Role of bolus in electron therapy

To date, conformal radiotherapy has been primarily photon conformal therapy, and it has been achieved by the use of multiple shaped fields, with and without intensity modulation. Photon conformal therapy can be used in treating tumors located throughout the body. However, because of the finite range of electrons in tissue, it may be advantageous to treat superficial tumors with electron conformal radiotherapy (ECRT), which is usually achievable using a single field. Because of the physical nature of the electron beam, its use for conformal therapy must be considered differently from that of the photon beam. Electron beams of energies ranging from 6 to 25 MeV are limited to treating target volumes within approximately 7.5 cm of the patient surface. Hence, ECRT seems best suited to treating superficial target volumes in head-and-neck and chest wall sites in which electron beams can be modified to deliver a uniform dose to the target volume, with a sharp dose falloff outside the volume. Although ECRT can also be achieved with moving electron beams, this paper will be limited to fixed-beam ECRT (1).

The American Association of Physicists in Medicine Task Group 25 recommends that electron beam parameters, such as energy, field size, and bolus, be selected so that the target volume is encompassed within 90% (or any other appropriate minimum dose) of the prescribed dose (2). At M. D. Anderson Cancer Center, our goal is to encompass the planning target volume (PTV) within 90% of the given dose. Given dose is the maximum central axis dose delivered in a water phantom at the same source-to-surface distance (SSD) and with the smallest rectangular field that encompasses the irregular field used on the patient (3). In ECRT, the goal is to select the optimal conditions to conform the 90% dose contour to the distal border of the target volume, while simultaneously maintaining as uniform dose within the PTV and as little dose to nearby critical organs and normal tissue as possible. In an actual patient, tumor underdose, normal tissue overdose, or nonuniform dose in the target volume can occur as a result of internal heterogeneities, an irregular patient surface, or a highly variable depth of the distal surface of the target volume (4). Hence, an electron beam with a spatially uniform energy and intensity is not always optimal. The solution to this problem

---

Reprint requests to: Rajat J. Kudchadker, Ph.D., Department of Radiation Physics, Box 94, The University of Texas M. D. Anderson Cancer Center, 1515 Holcombe Boulevard, Houston, TX 77030, USA. Tel: (713) 792-3230; Fax: (713) 745-0683; E-mail: rkudchad@mdanderson.org

is a beam that has higher energy where more penetration is necessary and a lower energy where less penetration is required. This can be achieved using electron bolus, which provides spatially dependent energy modulation of the electron field, thus compensating for the irregularities above.

Electron bolus has been defined by Hogstrom as "a specifically shaped material, which is usually tissue equivalent, that is normally placed either in direct contact with the patient's skin surface, close to the patient's skin surface, or inside a body cavity. This material is designed to provide extra scattering or energy degradation of the electron beam. Its purpose is usually to shape the dose distribution to conform to the target volume and/or to provide a more uniform dose inside the target volume" (5). In its application to conformal therapy, the primary goal is to select the minimal beam energy and optimal bolus design to conform to the 90% dose contour to the distal surface of the target volume so that there is minimal dose to nearby normal structures. In doing this, it is not always possible to maintain dose uniformity (i.e., 90%–100%) inside the PTV, because of multiple Coulomb scattering and variable source-to-surface distance (5).

Use of custom-shaped bolus to date

Use of custom-shaped bolus for electron therapy is not a new concept. Archambeau *et al.* described a bolus technique to be used with chest wall electrons that controlled the penetration of the electron beam over a large area (6). Beach *et al.* also described a bolus technique based on ultrasound and limited computed tomography (CT) images (7). Both of these techniques ignored the effects of electron scatter and also lacked the sophistication of accurate dose calculation, automated bolus design, and automated bolus fabrication. In previous work at M. D. Anderson, Low *et al.* (8) and Starkschall *et al.* (9) introduced a methodology based on patient CT data that allowed alteration of the dose distribution using bolus operators and a three-dimensional (3D) implementation of the pencil-beam algorithm. Low *et al.* also demonstrated the potential of an electron bolus in reducing the dose to uninvolved critical structures in treatment of the nose, parotid gland, and paraspinal muscles (8, 10). Perkins *et al.*, also from M. D. Anderson, demonstrated the utility of customized 3D electron bolus for optimizing postmastectomy irradiation of two patients with abnormal anatomy (11). As part of a project to establish a method for quality assurance of a milled electron bolus, Bawiec studied the design and fabrication of electron bolus for 9 patients, the majority with head-and-neck tumors (12).

Generally, it is desirable to have a uniform dose within the target volume, with the ratio of minimal to maximal dose not exceeding 90%, i.e., a dose variation within the target volume of 10% or less (13). Because the PTV includes the gross tumor volume, potential areas of local and regional microscopic disease around the tumor—and some normal tissue—hot spots inside the normal tissue, or cold spots inside the clinical tumor volume, should be minimized. In all of the studies described above, it was observed

that after using bolus to conform the distal 90% dose surface to the distal surface of the PTV, the dose spread in the PTV increased from the 10% (90%–100%) normally found in a water phantom to as much as 20%. This is attributed to the variation in the distance from the virtual source to the bolus surface (i.e., irregular shape of the bolus surface). Surface irregularities (patient or bolus surface), when compared to that for perpendicular incidence to a flat surface, increase nonuniformity of the dose distribution in the PTV, because of effects of inverse-square and because of loss of side-scatter equilibrium. It is well known that as the SSD decreases (increases), the value of maximum dose increases (decreases) (2). For example, if the thickness of a bolus is about 2.5 cm near the central axis, this increases the dose by about 5%. Also, it is a known fact that nonperpendicular incidence impacts depth–dose and that an irregular surface leads to hot and cold spots (4).

Purpose of current work-proof of principle

It should be possible to eliminate the excess dose nonuniformity caused by the bolus by modulating the incident electron fluence. It is our hypothesis that the degree of nonuniformity of the dose distribution, caused by the irregularly shaped proximal bolus surface, can be minimized by modulating the spatial distribution of the electron beam intensity. This will be shown possible by demonstrating for three different patient cases the ability to track the 90% dose surface to the distal surface of the PTV while simultaneously maintaining a dose uniformity of nearly 10% (90%–100%) throughout the PTV.

Although methods of delivering intensity-modulated electron beams have been discussed using multileaf collimators (MLCs) (14, 15) or scanned beams (16), this technology is not presently available for patient use. This work will demonstrate a potential use for electron intensity modulation using MLC once it becomes available in the clinic.

METHODS AND MATERIALS

In the present work, the benefit of using intensity modulation in conjunction with energy modulation using bolus will be demonstrated for a rectangular-shaped PTV in water and for three patients selected from a patient database developed by Bawiec (12). For each patient, two treatment plans are compared, one using bolus (energy modulation) and one using bolus and incident intensity modulation. The methodology described below will be followed for the water example and for each patient.

Principles of intensity-modulated bolus therapy

Electron bolus was first designed and optimized using the operator techniques explained by Low *et al.* (8). The bolus operators of Low *et al.* attempt to meet the following three criteria: adequate dose delivery to the PTV, avoidance of critical structures, and minimal dose heterogeneity within the PTV (8). The design of bolus is based upon three classes of operators: bolus creation, modification, and extension
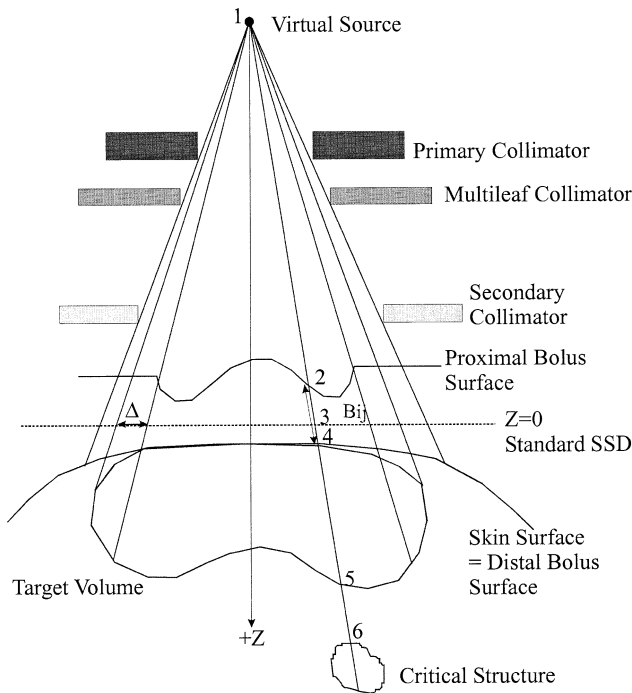
Fig. 1. Sketch illustrating the fan geometry and design elements of the bolus design system.

Fig. 2. Schematic representation of the bolus design fan grid intersecting a plane perpendicular to the central axis at the iso-center. The outer solid curve indicates the fan projection of the edge of the electron field size, whereas the dashed line indicates the projection of the lateral extent of the PTV. The dotted line represents the projection of the portion of the PTV used in designing bolus, defined by an area a distance Δ inside the lateral extent of the PTV. The fan lines within the dotted contour are indicated by a matrix of dots.

operators. The bolus is designed such that a prescribed isodose (e.g., 90% of the given dose) tracks the distal surface of the PTV while simultaneously attempting to maintain a dose distribution in the PTV as uniform as possible.

To further improve dose uniformity in the PTV while simultaneously tracking the prescribed isodose to the distal surface of the PTV, the electron pencil-beam weights can be varied once the bolus has been designed. Based on the variation of the electron pencil-beam weights, a "modulate intensity" operator was introduced to the initial list of operators. Presently, the "modulate intensity" operator is independent of how intensity modulation might be achieved. Also, the present intensity modulation is determined using only dose data along a single fan line. Because electrons scatter, and dose to a single point is dependent upon the intensity of many nearby fan lines, the methodology used here is not expected to provide the optimal solution. However, because the designed bolus surface and resulting dose variation are smooth, the present method results in a relatively smooth variation in intensity that, although not optimal, illustrates a possible solution and proof of principle.

A schematic representation of the bolus design fan grid (a plane containing the beam's central axis) is shown in Fig. 1. In Fig. 1, the design elements of the bolus are illustrated through the representation of one fan line on which points 1–6 are delineated (8). Point 1 represents the virtual electron source. Points 2–6 represent the intersections of the fan line with the proximal bolus surface, the standard SSD plane (shown by the dashed line), the proximal patient surface, the
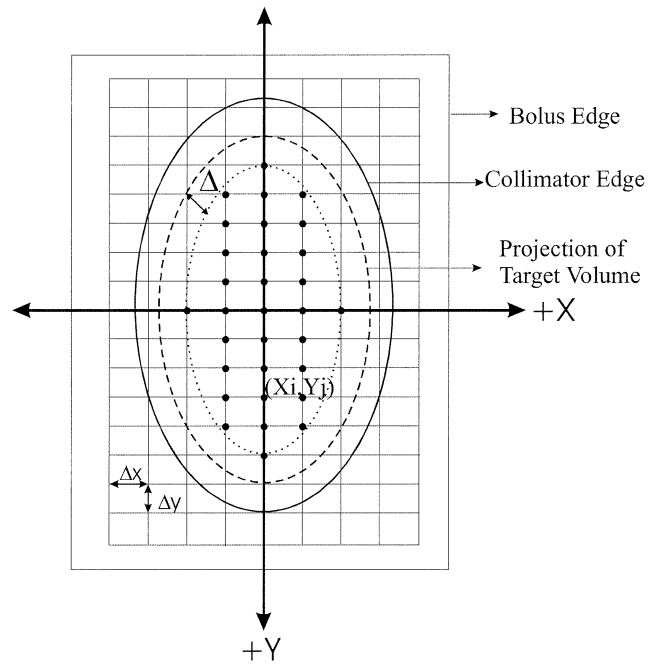
distal target volume surface, and the proximal critical structure surface, respectively.

Figure 2 shows the schematic representation of the bolus fan grid intersecting a plane perpendicular to the central axis at the isocenter. The outer solid curved line indicates the fan projection of the edge of the electron field size, usually defined by an applicator insert or "cutout"; the dashed line indicates the projection of the lateral extent of the PTV. Normally, an electron bolus would be designed over the entire target. However, because most target volumes have edges that tend to slope toward the surface, this would lead to boluses with steep gradients around the edges of the target volume. Therefore, the bolus design region is reduced by a bolus margin Δ. The inner dotted line (cf. Fig. 2) represents the projection of the portion of the PTV used in designing bolus, defined by an area a distance Δ inside the lateral extent of the PTV. The fan lines within the dotted contour are indicated by a matrix of dots. The bolus design operators (creation and modification), as well as the "modulate intensity" operator, are allowed to operate only on these points. The intensity modulation was limited to the region, because we wanted to avoid correcting tumor underdoses due to inadequate margin between the PTV and field edge.

Once the bolus has been designed using a sequence of bolus design operators, the maximum value of dose along

each fan line at least a distance Δ inside the PTV is determined. The desired intensity of the electron beam is determined based on the goal of achieving a constant maximum dose along each fan line. To achieve this, the initial pencil-beam weight along each fan line is multiplied by a ratio of the desired constant maximum value of dose, e.g., 100% of the given dose, to the maximum value of dose (expressed as a percentage of the given dose) along that fan line. For the fan lines just outside the dotted contour in Fig. 2 (the region Δ, where the "modulate intensity" operator is not designed to operate), the initial beam weights before intensity modulation are used. It should be noted here that, in using these two sets of beam weights, inside (modulated beam weights) and outside (initial beam weights) the dotted contour, might give rise to nonsmooth regions near the field boundary in the final intensity profile. Now, using these pencil-beam weights, the dose is recomputed. In this manner, the "modulate intensity" operator tries to maintain a uniform dose distribution (e.g., 90%–100% of given dose) within the target volume. For example, if a hot spot of 110% is present along a certain fan line within the PTV, the beam weight along that fan line is reduced to 0.909 of its original value, thus giving rise to a more homogeneous final dose distribution. To control the amount of intensity modulation, the minimum and maximum electron pencil-beam weight limits have been set to 0.8 and 1.2, respectively. However, it should be noted that in all cases studied in the present work, the pencil-beam weights remained well within these limits. To achieve intensity values greater than 100% requires the monitor units to increase, and to achieve intensity modulation requires a dynamic MLC or other technology. The resulting total monitor units and MLC movement depend upon the particulars of the MLC and method of variation.

The pencil-beam weights are manipulated to achieve a more homogeneous dose distribution in the target volume in the presence of bolus while maintaining the sharp dose falloff external to the volume; however, because the intensity operator is introduced, prior dose (e.g., 90%) along the distal end of the PTV may have increased or decreased. To restore the 90% isodose line to conform to the distal surface of the PTV, bolus operators such as the shift isodose operator and the smoothing operator must be used after application of the intensity operator, i.e., after the bolus shape is redesigned. These final bolus modifications are usually small, because modifications to the intensity are minimal (<20%).

Design of bolus

Initially, a 3D patient data set composed of a set of transverse CT slices and outlines of the PTV and other critical organs are extracted from the Bawiec data set (12). After the selection of a suitable electron beam energy, SSD, field size, and other variables, bolus is designed using a sequence of operators defined by Low *et al.* (8). This is done using COPPERPlan, a treatment-planning system we developed in-house that uses a 3D implementation of the electron pencil-beam algorithm to calculate dose (9, 17, 18).

The three classes of operators for bolus design are the following: creation, modification, and extension (8). We have used the physical depth creation operator $P(\Delta, R_{90})$ for initial bolus creation. This operator forces the sum of bolus thickness and physical depth of the PTV to equal R_{90} along each fan line that lies a distance Δ inside the PTV (cf. Fig. 2). To refine the bolus design, we apply a sequence of operators taken from our set of modification operators, e.g., $I(R_{90})$, isodose shift; $S_t(\eta,\mu)$, Gaussian thickness smoothing; $S_h(\eta,\mu)$, Gaussian height smoothing; $T(\eta)$, maximum PTV coverage; and $C(\eta,D_c)$, critical structure avoidance. The bolus thickness was extended outside the collimator edge (cf. Fig. 2) using the constant height extension operator H_h. These operators were applied sequentially and could be applied more than once during the bolus design process, if necessary. After the electron bolus was designed, the dose distribution was computed and examined. To eliminate any hot or cold spots that might have been generated from the introduction of the bolus, the "modulate intensity" operator, M, was applied. As a result, dose in regions along the distal end of the target volume was either reduced or increased. To correct for this, the bolus was redesigned using the isodose shift operator, $I(R_{90})$, and the Gaussian height-smoothing operator, $S_h(\eta,\mu)$. Because the operators each address a single dosimetric issue, they can adversely affect other attributes of the dose distribution. However, with experience the treatment planner can apply these operators in sequences that generate acceptable dose distributions.

Patient example: Chest wall, postmastectomy case

The first patient example deals with the irradiation of the chest wall. This patient is a 62-year-old woman who underwent a left modified radical mastectomy for breast cancer and later had a recurrence along the caudal medial portion of her scar (12). She was noted to have two separate nodules of recurrent tumor. The superior and deep margins were positive at resection. The deep margin was converted to negative by partial resection of ribs 5 and 6. This patient was selected for this study, because the highly variable thickness of the chest wall would cause needless irradiation of portions of the lung and heart without the use of electron bolus.

The skin surface and the general location of the distal surface of the PTV were at an angle of 35° with respect to a surface perpendicular to the anterior-posterior direction. Therefore, a gantry angle of 35° was selected for the electron beam, placing the distal surface of the PTV approximately perpendicular to the beam's central axis. The maximum depth of the PTV was determined to be 2.3 cm. An electron beam with a nominal energy of 9 MeV was chosen, because this beam has an R_{90} of 2.6 cm for the field size chosen. The lateral surfaces of the PTV were approximately parallel to central axis. Hence, the tracing of the treatment portal required a 1.5-cm margin (defined at isocenter) around the projection of the greatest lateral extent of the PTV to account for constriction of the 90% dose surface and

Table 1. Operator sequence and parameters used for each patient case

Patient site	Operator sequence and parameters
Chest wall: Postmastectomy	1. Bolus margin (Δ): $\Delta = 0.50$ cm 2. Bolus depth ($P[\Delta, R_t]$): $\Delta = 0.50$ cm, $R_t = R_{90} = 2.3$ cm 3. Maximum target coverage operator ($T[\eta]$): $\eta = 1.0$ 4. Smoothing heights ($S_h[\eta, \mu]$): $\eta = 100.0$, $\mu = 1.0$ 5. Isodose shift ($I[R_t]$): $R_t = R_{90} = 2.3$ cm 6. Smoothing heights ($S_h[\eta, \mu]$): $\eta = 100.0$, $\mu = 1.0$ 7. Intensity modulation (M) 8. Isodose shift ($I[R_t]$): $R_t = R_{90} = 2.3$ cm 9. Smoothing heights ($S_h[\eta, \mu]$): $\eta = 100.0$, $\mu = 1.0$ 10. Bolus extension (H_h): perpendicular to the beam
Thorax: Paraspinal muscles	1. Bolus margin (Δ): $\Delta = 0.50$ cm 2. Bolus depth ($P[\Delta, R_t]$): $\Delta = 0.50$ cm, $R_t = R_{90} = 5.7$ cm 3. Smoothing heights ($S_h[\eta, \mu]$): $\eta = 1.0$, $\mu = 1.0$ 4. Intensity modulation (M) 5. Bolus extension (H_h): perpendicular to the beam
Head and neck: Right buccal mucosa	1. Bolus margin (Δ): $\Delta = 0.50$ cm 2. Bolus depth ($P[\Delta, R_t]$): $\Delta = 0.50$ cm, $R_t = R_{90} = 7.1$ cm 3. Smoothing heights ($S_h[\eta, \mu]$): smoothing surface $\sigma = 1.0$, weight $= 1.0$ 4. Isodose shift ($I(R_t)$): $R_t = R_{90} = 7.1$ cm 5. Smoothing heights ($S_h[\eta, \mu]$): $\eta = 1.0$, $\mu = 1.0$ 6. Intensity modulation (M) 7. Isodose shift ($I(R_t)$): $R_t = R_{90} = 7.1$ cm 8. Smoothing heights ($S_h[\eta, \mu]$): $\eta = 1.0$; $\mu = 1.0$ 9. Bolus extension (H_h): perpendicular to the beam

to ensure complete coverage of the PTV. The sequence of bolus operators used for this plan is given in Table 1.

Patient example: Thorax, paraspinal muscles case

The second bolus design example deals with the irradiation of the paraspinal muscles. This patient is a 19-year-old woman with a diagnosis of chondrosarcoma in the paraspinal area (12). The mass extended from thoracic vertebrae 9–11 and measured 11 cm superior-to-inferior by 6.5 cm laterally. The PTV measured 19 cm superior-to-inferior by 12.9 cm laterally. The depth from the patient skin surface to its distal surface varied from 2.0 cm to 5.8 cm. The patient was selected for this study because of this variation in depth to the distal surface of the PTV, to attempt to protect the spinal cord, right lung, and right kidney from excess dose. An electron beam with a nominal energy of 20 MeV was chosen, because this beam has an R_{90} of 6.0 cm for the field size chosen. Because the PTV was approximately parallel to the skin surface in the midsagittal plane, the table angle was rotated 90° to allow for a gantry angle of 7°, placing the distal surface of the PTV approximately perpendicular to the central axis of the electron beam. The treatment portal was designed by tracing a 1.5-cm margin around the projection of the greatest lateral extent of the PTV in a beam's-eye–view. The sequence of bolus operators used for this plan is given in Table 1.

Patient example: Head-and-neck, right buccal mucosa case

This third bolus design example deals with the irradiation of the right buccal mucosa and surrounding areas. This patient is a 65-year-old female with a diagnosis of squamous cell carcinoma in the right buccal mucosa (12). The mass measured 8.5 cm $\times$ 4.0 cm $\times$ 4.0 cm. The mass invaded both the mandible and maxilla and displaced the masseter and medial pterygoid. Treatment consisted of resection followed by postoperative irradiation. The patient was selected for this study because of the underlying spinal cord and because her facial defects, which resulted from surgical procedures, created a nonuniform surface. A gantry angle of 10° was used for this patient. The maximum depth of the distal surface of the PTV was 7.1 cm; therefore, an electron beam with a nominal energy of 25 MeV was chosen, because this beam has an R_{90} of 7.1 cm for the field size chosen. The treatment portal was designed by tracing a 2-cm margin around the projection of the greatest lateral extent of the PTV in a beam's-eye–view. The sequence of bolus operators used for this plan is given in Table 1.

Normalization of dose and method for comparing plans

The electron-dose distribution was calculated with the designed bolus included in the computation. The dose calculation generates a file of doses per unit beam weight. To combine beams for calculation of a treatment plan, beam weights must be assigned. For the first two patients, there was no danger of the bolus colliding with the electron applicator. Hence, the patients were planned with an SSD of 100 cm to the patient's skin surface (not to the proximal bolus surface), and the beam weight was set to 100. For the patient with the buccal tumor, the bolus would have collided with the electron applicator if an SSD of 100 cm were used. Hence, this patient was planned with an SSD of 105 cm to
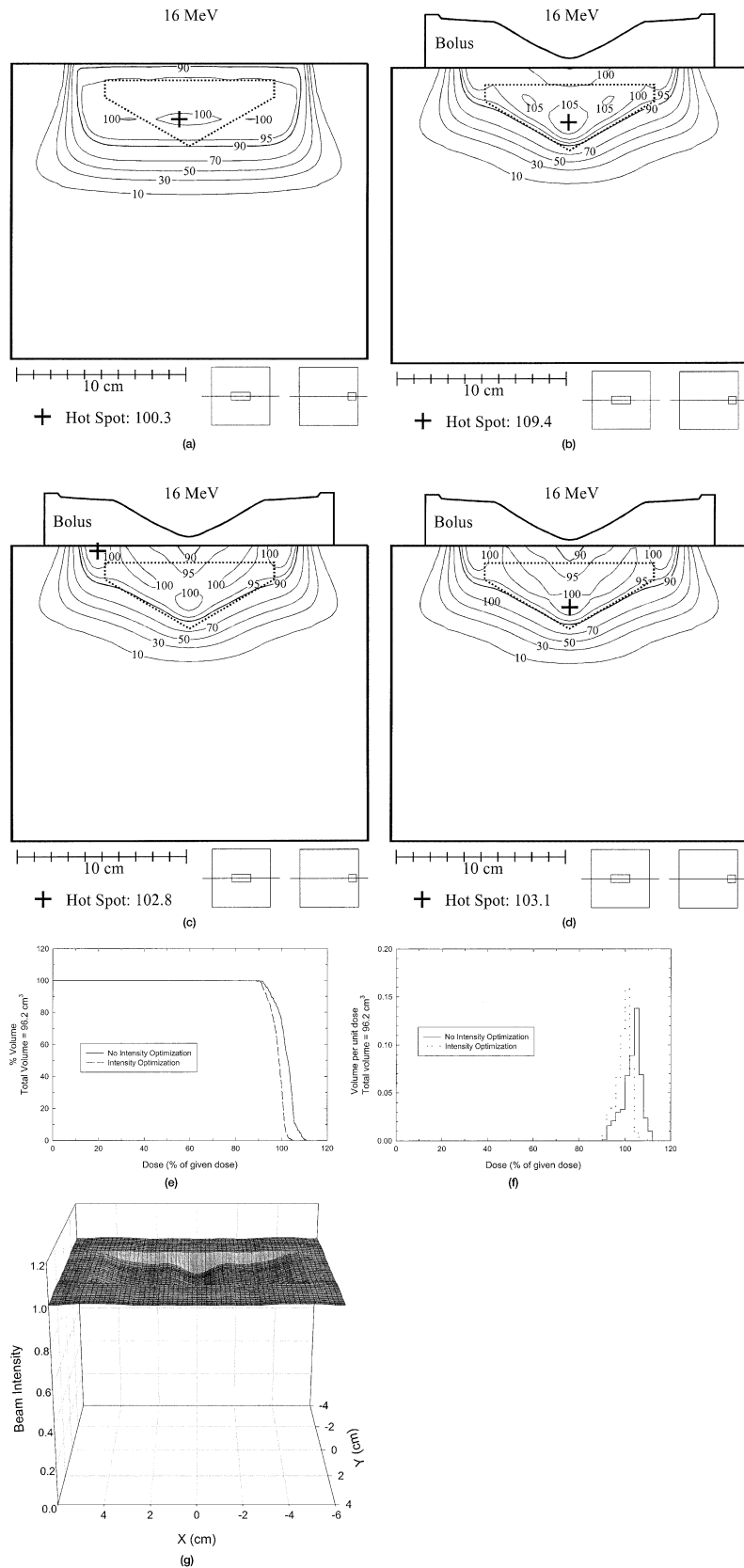
Fig. 3. Dose distributions for the hypothetical target volume case. PTV is delineated by the dashed line. An electron energy of 16 MeV was used in all cases. The variation in dose distribution for cases is representative of the following: (a) with no electron bolus, (b) with electron bolus, (c) with intensity modulation and bolus, (d) with intensity modulation and modified bolus, (e) comparison of cumulative DVHs for cases with and without intensity modulation, (f) comparison of differential DVHs for cases with and without intensity modulation, and (g) intensity profile after modulation.
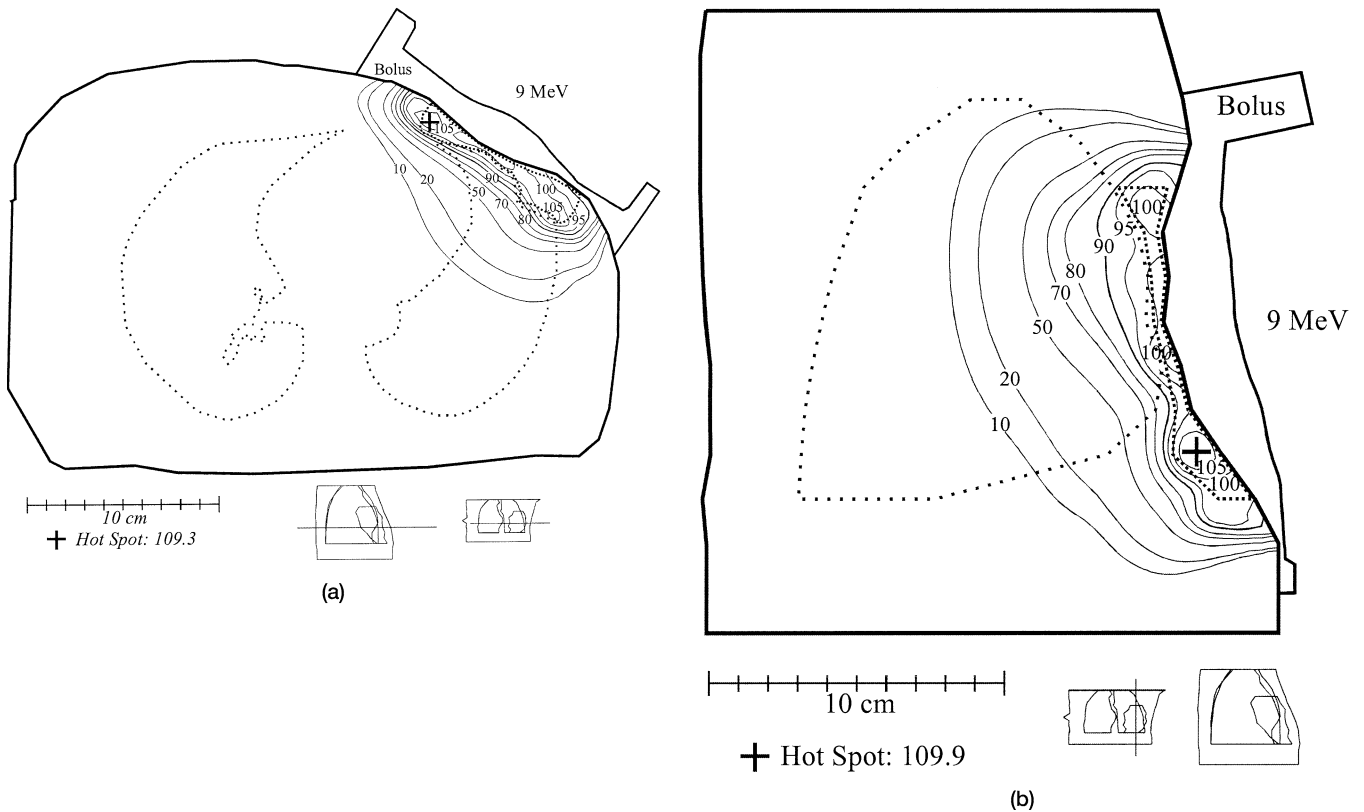
Fig. 4. Isodose distribution (%) for the postmastectomy chest wall case before intensity modulation. The treatment volume is delineated with the dashed contour (a) transverse slice, (b) sagittal slice.

the patient's skin surface, and the beam weight was set to 110.25 to account for inverse square. The resulting dose is the product of the beam weight and the dose per beam weight calculated by the pencil-beam algorithm. In all cases, the PTV has been prescribed to a minimum dose of 90% of the given dose. To help appreciate the improvement in using intensity modulation, the planar dose distribution with intensity modulation is compared with that without intensity modulation in two orthogonal representative planes for each patient. To appreciate the impact in 3D, dose–volume histograms (DVH) are compared for the PTV.

RESULTS

Simulated results in a water phantom

To illustrate the process of intensity-modulated bolus therapy, Fig. 3 shows simulated results of a water phantom with a hypothetical PTV 10 cm in length and of constant cross-section (with a shape similar to a baseball field's home plate). The distal PTV surface has been drawn with sloping edges, with a depth of 5.0 cm at the deepest point. A 16-MeV electron beam was used with a collimator setting of $9 \times 15 \ cm^2$. Our goal was to achieve a minimum dose of 90% of the given dose to the entire PTV while limiting the dose to any existing critical structures lateral or distal to the PTV. In Fig. 3a, the isodose distribution is shown for the case of no electron bolus. As seen in the figure, the PTV is

covered by the 90% isodose, and the dose variation is 10% (90%–100%). However, a significant volume of healthy tissue outside the PTV is being exposed to unnecessary dose (>90%). With the introduction of a suitably designed electron bolus, as shown in Fig. 3b, the 90% isodose line now follows the distal boundary of the PTV, minimizing dose to healthy tissue outside the PTV. The surface dose has also increased, as expected, because of the presence of the bolus. The irregular proximal bolus surface, because of inverse square and scatter effects, increases the dose spread to 19% (90%–109%). This increased dose spread can be reduced by intensity modulation of the electron beam using the "modulate intensity" operator. Figure 3c shows the dose distribution after applying the "modulate intensity" operator, resulting in a more homogeneous dose distribution in the PTV; i.e., maximum dose decreased from 109% to 103%. However, the dose to the distal tumor surface drops proportionally, so that the 90% dose surface now under-irradiates the distal surface of the PTV. To restore the conformity, the bolus top surface is modified slightly to shift the 90% dose surface to again match the distal surface, the resulting dose distribution shown in Fig. 3d. In Figs. 3e and 3f, the PTV cumulative DVH and differential DVH for the plan with bolus (energy modulation) only (Fig. 3b) is compared with that for the plan with bolus and intensity optimization (Fig. 3d), respectively. When comparing the bolus with no intensity modulation case to the bolus with intensity modulation
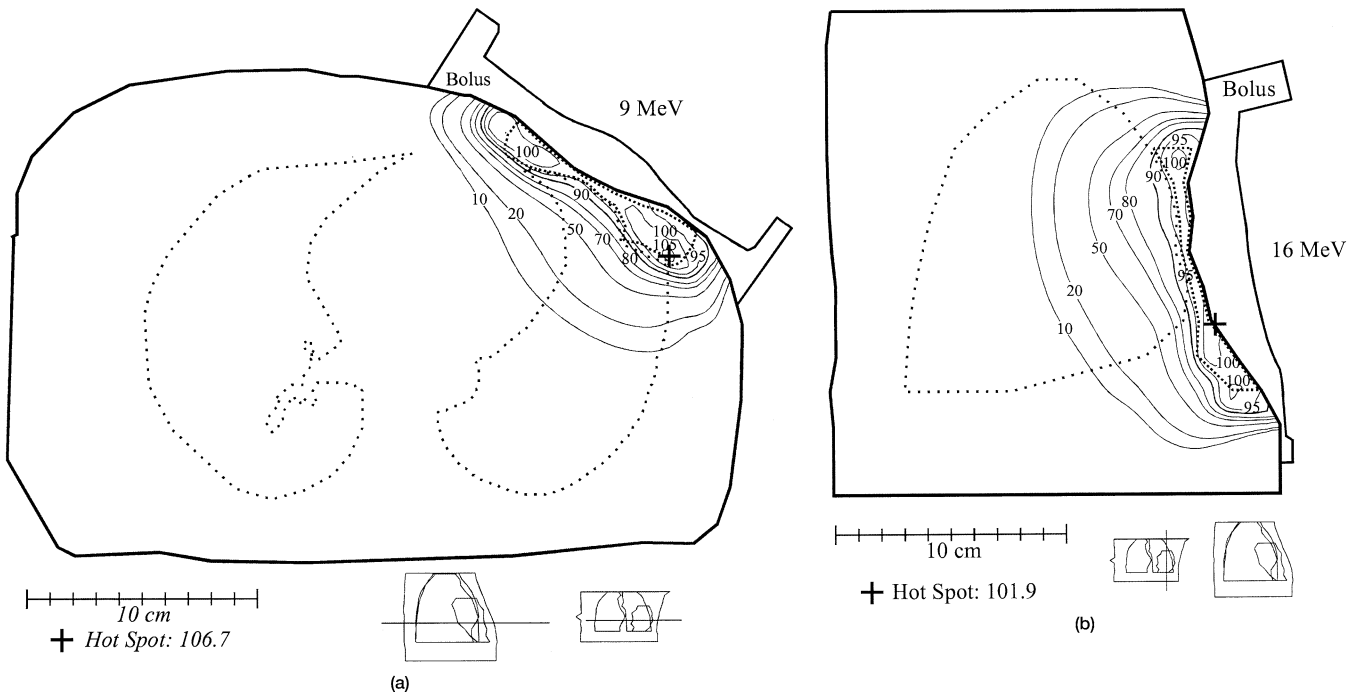
Fig. 5. Isodose distribution (%) for the postmastectomy chest wall case after intensity modulation. The treatment volume is delineated with the dashed contour (a) transverse slice, (b) sagittal slice.

case, the first observation in Fig. 3e is that the maximum dose is reduced from 110.9% to 104.6%. More significantly, the $\Delta D_{90\%-10\%}$ was reduced from 10.4% to 7.8%, a reduction of 2.6%. The differential DVH in Fig. 3f shows a decrease in dose spread and a decrease in maximum dose when comparing the bolus with no intensity modulation case to the bolus with intensity modulation case. The beam intensity designed by the intensity optimization operator is shown in Fig. 3g, varying from 91.5% to 102%. This example indicates how a modified electron bolus incorporating the beam intensity modulation can be used to generate a more optimal ECRT technique for the treatment of superficial target volumes.

Chest wall: Postmastectomy case

For the designed bolus without intensity modulation, Fig. 4a shows the dose distribution in a transverse plane, and Fig. 4b shows it in a sagittal plane. In both planes, the 90% isodose contour contains the PTV, which is delineated by the dotted line. In this patient, the depth of the PTV was less in the central region and more in the periphery. Therefore, the designed bolus was thicker in the central region than along the periphery, to compensate for the varying thickness of the PTV. The thickness of the bolus near the central axis is about 2.5 cm, and as a result of inverse square, increases the dose by about 5%. Additionally, the sloping walls of the bolus focused scattered electrons toward the periphery of the PTV, thus contributing increased dose in the target volume, i.e., giving rise to the hot spots and increasing the maximum dose in the PTV. In Fig. 4a, hot spots are observed near the medial and lateral boundaries of the PTV in the transverse plane, the maximum being 109%.

Also, a hot spot of 110% is present in the inferior region of the PTV in the sagittal plane (cf. Fig. 4b). For the designed bolus with intensity modulation, Fig. 5a shows the dose distribution in a transverse plane, and Fig. 5b shows it in a sagittal plane. The hot spots that were present before the application of intensity modulation have been reduced, resulting in a more homogeneous dose distribution in the PTV. In Fig. 5a, the transverse view, a hot spot of 107% remains at the distal edge of the PTV. This is because it is outside the region where the "modulate intensity" operator was designed to operate. Recall that the reason for introducing this constraint into the algorithm is because near the target lateral boundaries, the PTV may be shallow and bolus thickness large. If this constraint were absent, the electron pencil-beam weights could ramp up to values too high near the boundaries of the PTV, making the delivery of the intensity-modulated beam impossible.

To better appreciate the improvement in dose homogeneity, Fig. 6 compares the DVH for the PTV with the bolus and no intensity modulation (solid curve) with the DVH for the PTV with the bolus and intensity modulation (dashed curve). The first observation is that the median dose decreased by 2.1%, from 101.4% to 99.3%. More significantly, the $\Delta D_{90\%-10\%}$ was reduced from 8.9% to 7.2%. The change in median dose is not particularly significant, because it could have been achieved by a change in beam weighting. The 1.7% reduction in dose spread is a direct result of intensity modulation, but it is not likely clinically significant. The intensity-modulated fluence profile of the incident beam is shown in Fig. 7. The variation in intensity is smooth and small, ranging from 88% to 101%.
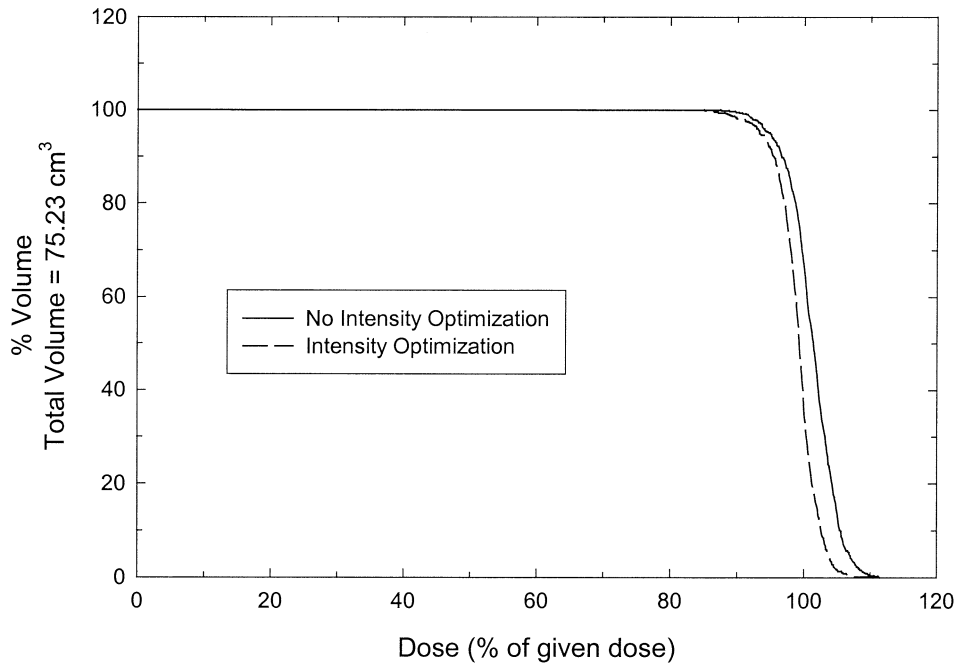
Fig. 6. Comparison of dose–volume histograms for the postmastectomy chest wall case before (solid line) and after (dashed line) intensity modulation.

Thorax: Paraspinal muscles case

For the designed bolus without intensity modulation, Fig. 8a shows the dose distribution in a transverse plane, and Fig. 8b shows it in a sagittal plane. In both planes, the 90% isodose contour encloses the PTV, which is delineated as the dotted line. The isodose plots suggest that the plan with the electron bolus and no intensity modulation would be adequate to treat this patient. Nonetheless, this case was studied to determine whether the islands of slightly higher dose, e.g., the 105-isodose lines seen in the sagittal view (cf. Fig. 8b) of the PTV, could be eliminated with intensity optimization. For the designed bolus with intensity modulation, Fig. 9a and Fig. 9b show the dose distribution in a transverse plane and sagittal plane, respectively. There is now a more homogeneous dose distribution in the PTV, evidenced by the islands of 105% isodose lines having been eliminated.
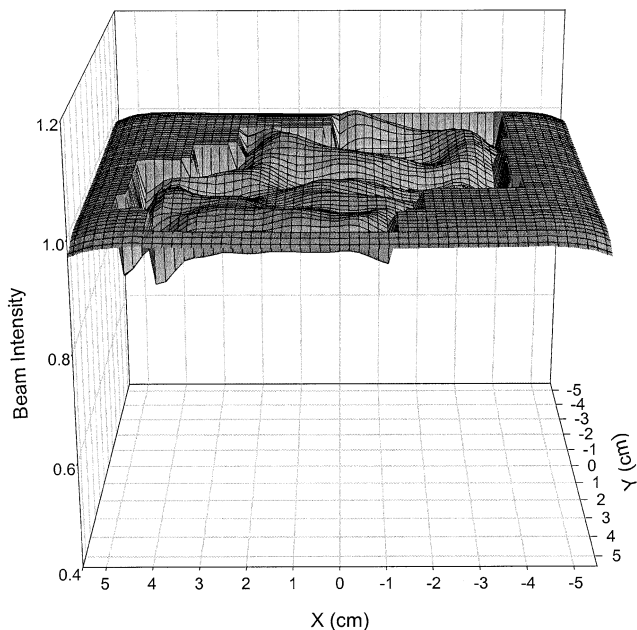
Again, to better appreciate the improvement in dose homogeneity, Fig. 10 compares the DVH for the PTV with the bolus and no intensity modulation (solid curve) with the DVH for the PTV with the bolus and intensity modulation (dashed curve). The first observation is that the median dose decreased by 2.5%, from 101% to 98.5%. More significantly, the $\Delta D_{90\%-10\%}$ was reduced from 8.2% to 5.7%. Again, the change in median dose is not particularly significant, because it could have been achieved by a change in beam weighting. The 2.5% reduction in dose spread is a direct result of intensity modulation, which again is not clinically significant. The intensity-modulated fluence profile of the incident beam is shown in Fig. 11. The variation in intensity modulation is smooth and small, ranging from 92% to 107%.

Head and neck: Right buccal mucosa case

For the designed bolus without intensity modulation, Fig. 12a shows the dose distribution in a transverse plane, and Fig. 12b shows it in a coronal plane. As seen in the coronal plane, the 90% isodose line misses a small portion of the PTV, delineated by the dotted line. This is in part because of

Fig. 7. Intensity profile after modulation for the postmastectomy chest wall case.
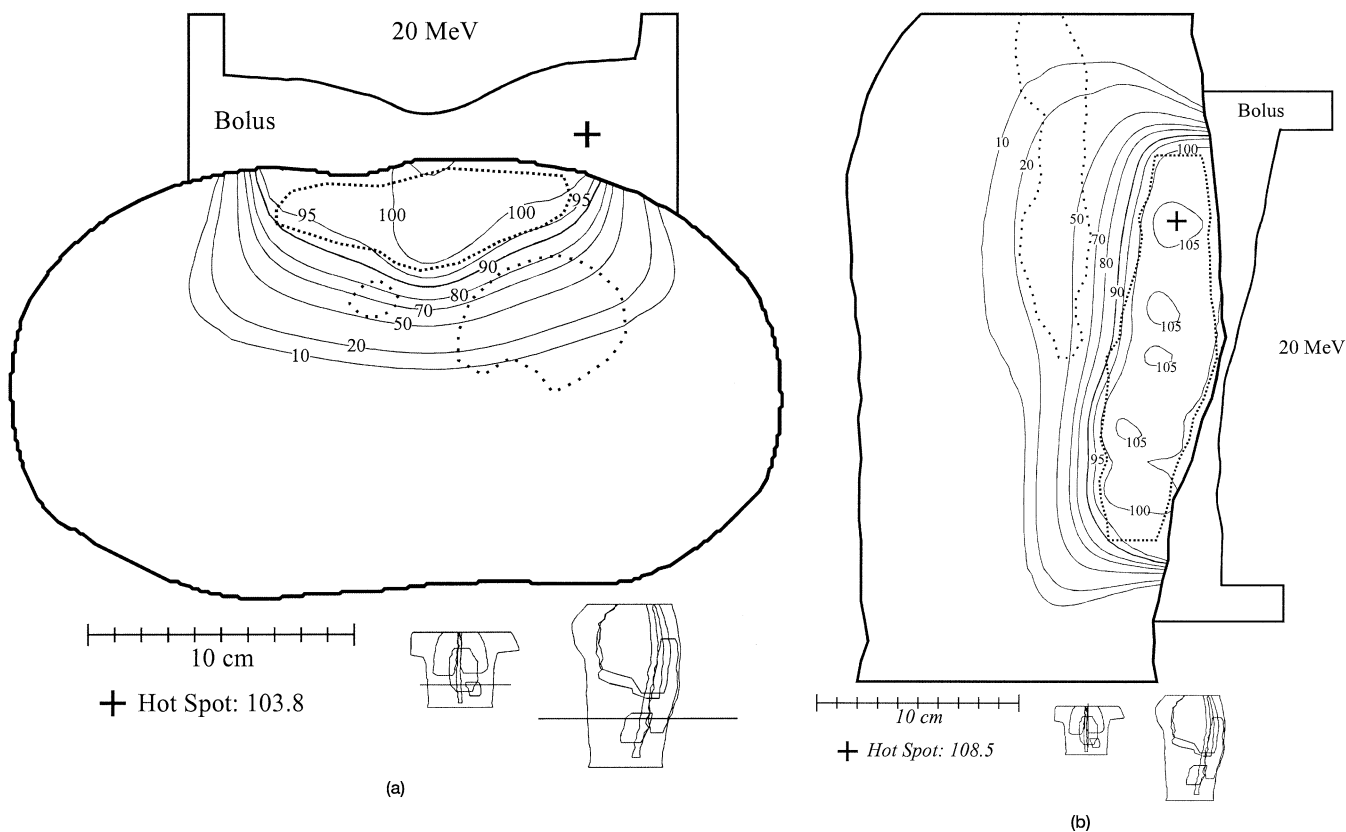
Fig. 8. Isodose distribution (%) for the thorax, paraspinal muscles case, before intensity modulation. The treatment volume is delineated with the dashed contour (a) transverse slice, (b) sagittal slice.

the irregularity in the contours along the distal PTV surface in consecutive transverse CT slices. The coronal view of the target volume (cf. Fig. 12b) shows a region of high dose. This hot spot is created by the steep gradient of the proximal bolus surface, which is necessary to conform the 90% dose surface to the sharp gradient in the distal surface of the PTV. Again, the dose inhomogeneity within the PTV is a result of the effects of inverse-square and electron scatter. For the designed bolus with intensity modulation, Figs. 13a and 13b show the dose distribution in a transverse plane and a coronal plane, respectively. There is now a more homogeneous dose distribution in the PTV, and the hot spot has been significantly reduced.

In Fig. 14, the solid curve shows the DVH for the PTV with the bolus and no intensity modulation, and the dashed curve shows the DVH for the PTV with the bolus and intensity modulation. The original bolus plan without intensity optimization has a maximum target dose of 120.2% and a mean target dose of 100.7%. After applying intensity modulation and modifying the bolus, the maximum target dose has been reduced substantially to 108.5% with a mean dose of 96.3%. In the nonoptimized plan, approximately 97.7% of the PTV received a dose in excess of 90% of the given dose, whereas approximately 94.7% of the PTV received this dose in the optimized plan. More significantly, the $\Delta D_{90\%-10\%}$ was reduced from 14.9% to 9.2%. Again, the reduction in dose spread is a direct result of intensity

modulation. The intensity modulation is minimal (81.5%– 107.3%) and is shown in Fig. 15.

DISCUSSION

The patient examples demonstrated that bolus with intensity modulation provides a more uniform dose to the PTV than bolus without intensity modulation. In patient cases where dose uniformity in the PTV is insufficient using only bolus, bolus with intensity modulation offers a solution to be added to the electron conformal therapy arsenal. The methodology for determining electron intensity used in the present work is simplistic, but yielded reasonably good results in improving PTV dose uniformity. More sophisticated methods, such as optimizing the intensity modification operator in the present system or performing optimization of pencil-beam weights, may further improve dose uniformity (15, 19); however, it is not clear that such techniques will be necessary.

The use of intensity modulation to improve dose homogeneity is potentially clinically significant in the head-and-neck example. This was not seen in the bolus without intensity modulation treatment plans for the chest wall and thorax, because the intensity modulation operation was limited to a small region inside the PTV. These results indicate that further improvement in deriving the intensity optimization may be possible and useful.
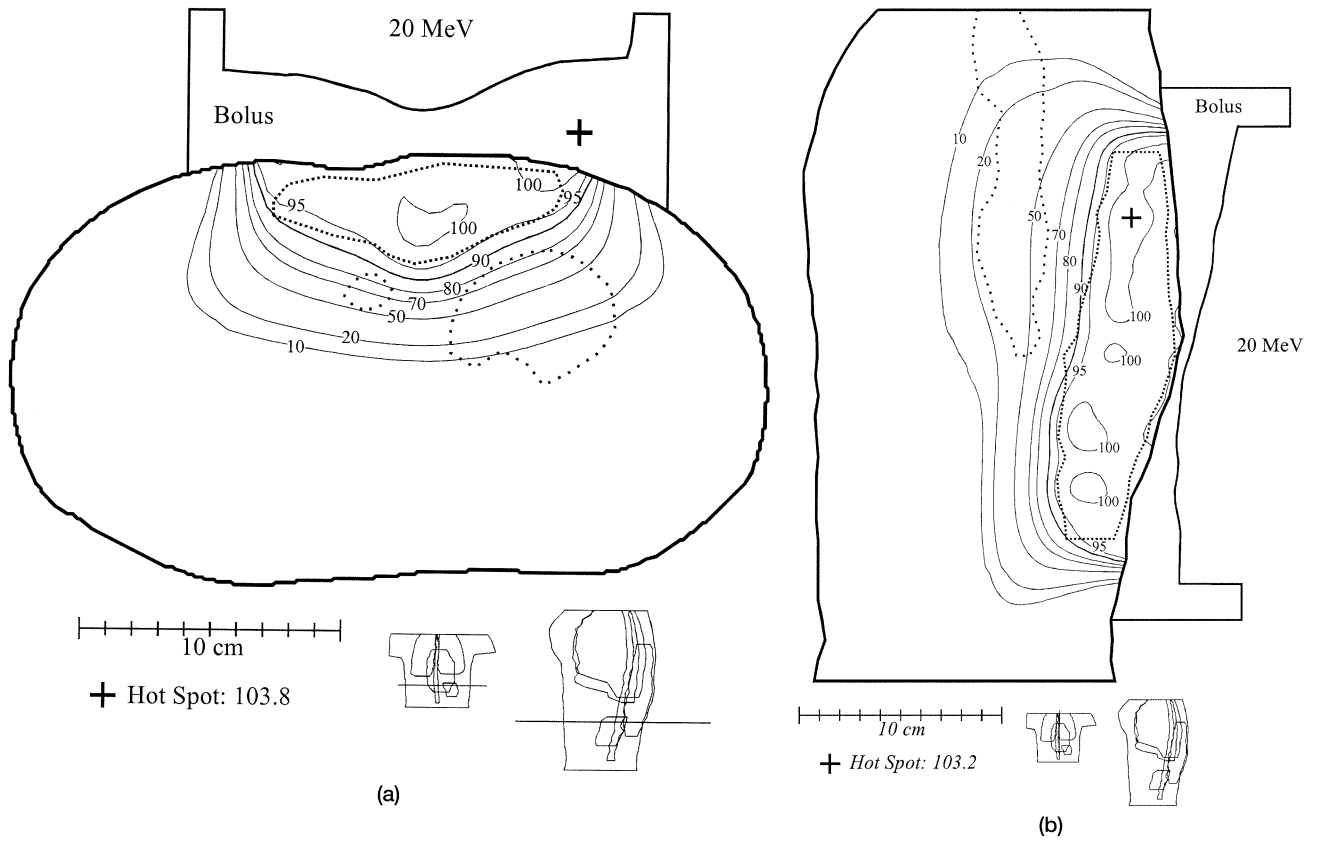
Fig. 9. Isodose distribution (%) for the thorax, paraspinal muscles case, after intensity modulation. The treatment volume is delineated with the dashed contour (a) transverse slice, (b) sagittal slice.

This procedure and the potential of intensity-modulated bolus therapy are illustrated in the present work. Evaluation of the clinical utility will require testing this procedure for a greater patient population and using an appropriate plan evaluation method in that process. Additionally, it will be necessary to determine the advantages and disadvantages of
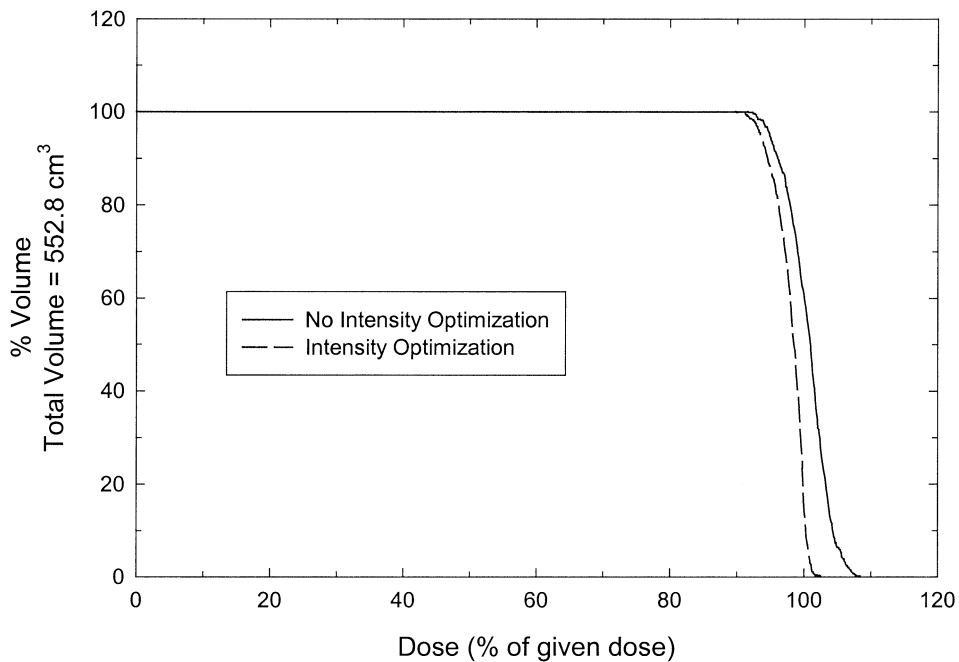
Fig. 10. Comparison of dose–volume histograms for the thorax, paraspinal muscles case, before (solid line) and after (dashed line) intensity modulation.
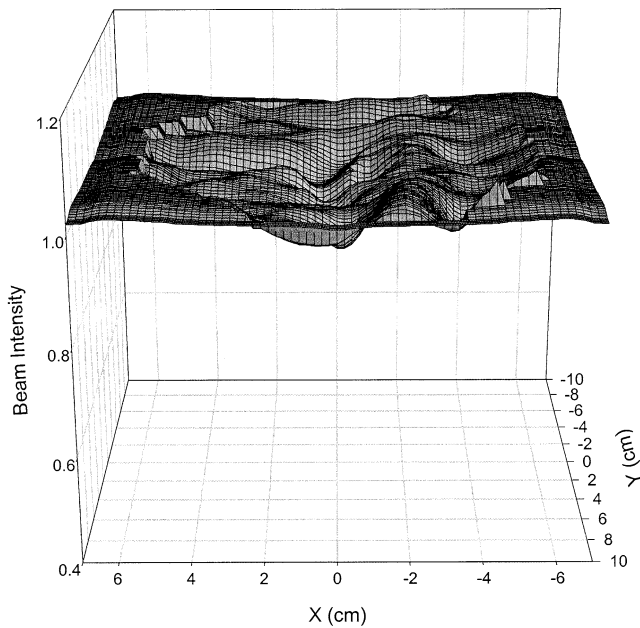
Fig. 11. Intensity profile after modulation for the thorax, paraspinal-muscles, case.

the present method compared with other methods that do not require electron bolus.

For this method to become available in the clinic will require the availability of methods for electron intensity modulation and for their inclusion in treatment-planning systems. Presently, there are at least three options for computer-controlled intensity modulation. One of the earlier methods has been that of intensity-modulated spot scanning (16). This method is not particularly attractive, because of the unavailability of computer-controlled scanned electron beams. Also, there is concern that the lateral spread of the spot beams might be too large at energies below 25 MeV, and the width of the pencil beams in the patient might be too large at the energies above 25 MeV. Both of these effects would impact the ability to achieve optimal dose uniformity.

The most attractive option is to use existing X-ray MLC to modulate the intensity of the electron beam. Using the X-ray MLC, which exists on many linear accelerators today, would be within the scope of a modern radiotherapy department. Dynamic multileaf collimation using the X-ray MLC can be used for modulating the electron fluence, similar to X-ray beam modulation (14). However, the large air gap between the X-ray MLC and patient may limit the resolution of intensity modulation, again because of the large lateral spread of a pencil beam that originates at the MLC (20). This leads to unacceptably large penumbra in the patient plane, so that an electron applicator with cutout will still be required for field shaping. Moran *et al.* have shown
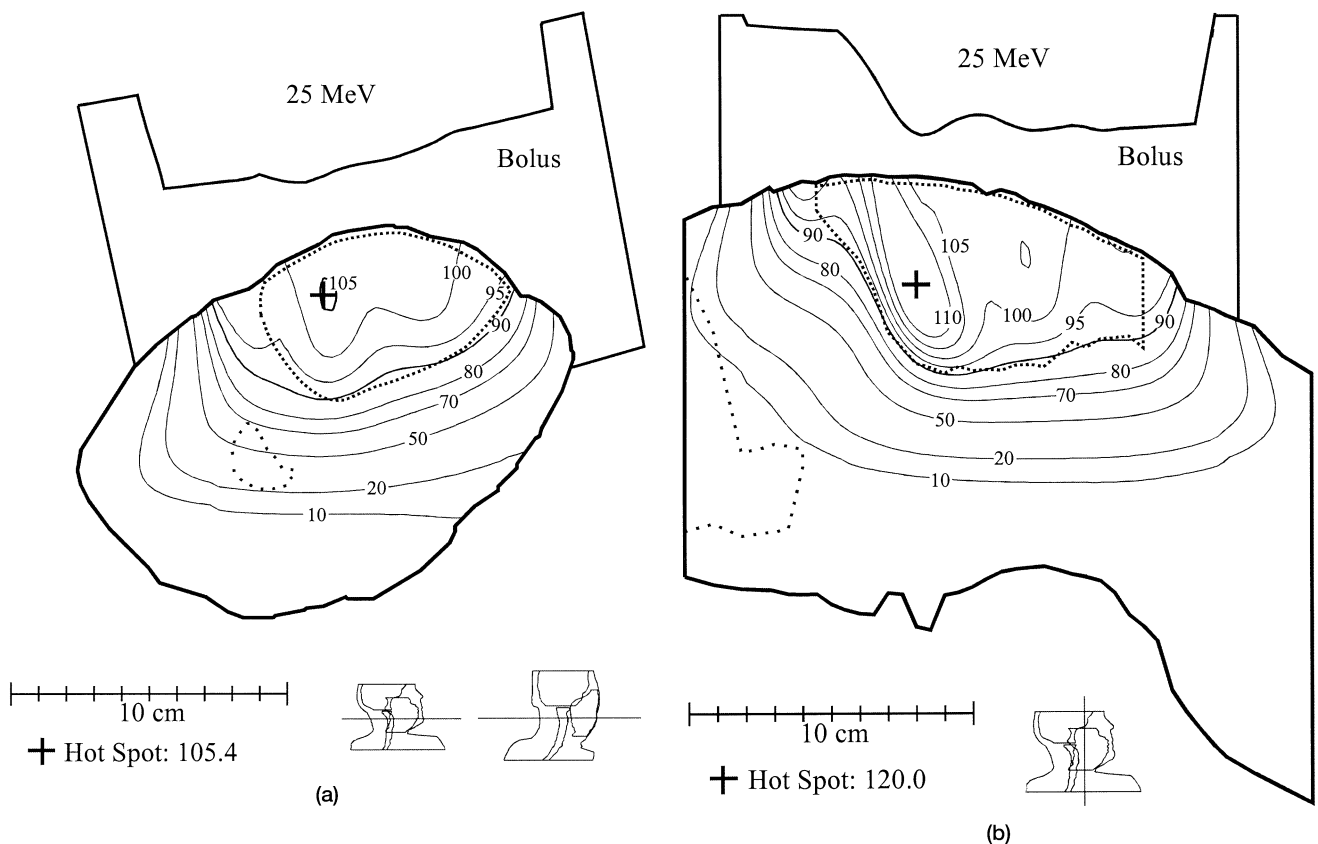

Fig. 12. Isodose distribution (%) for the head-and-neck, right buccal mucosa case, before intensity modulation. The treatment volume is delineated with the dashed contour (a) transverse slice, (b) coronal slice.
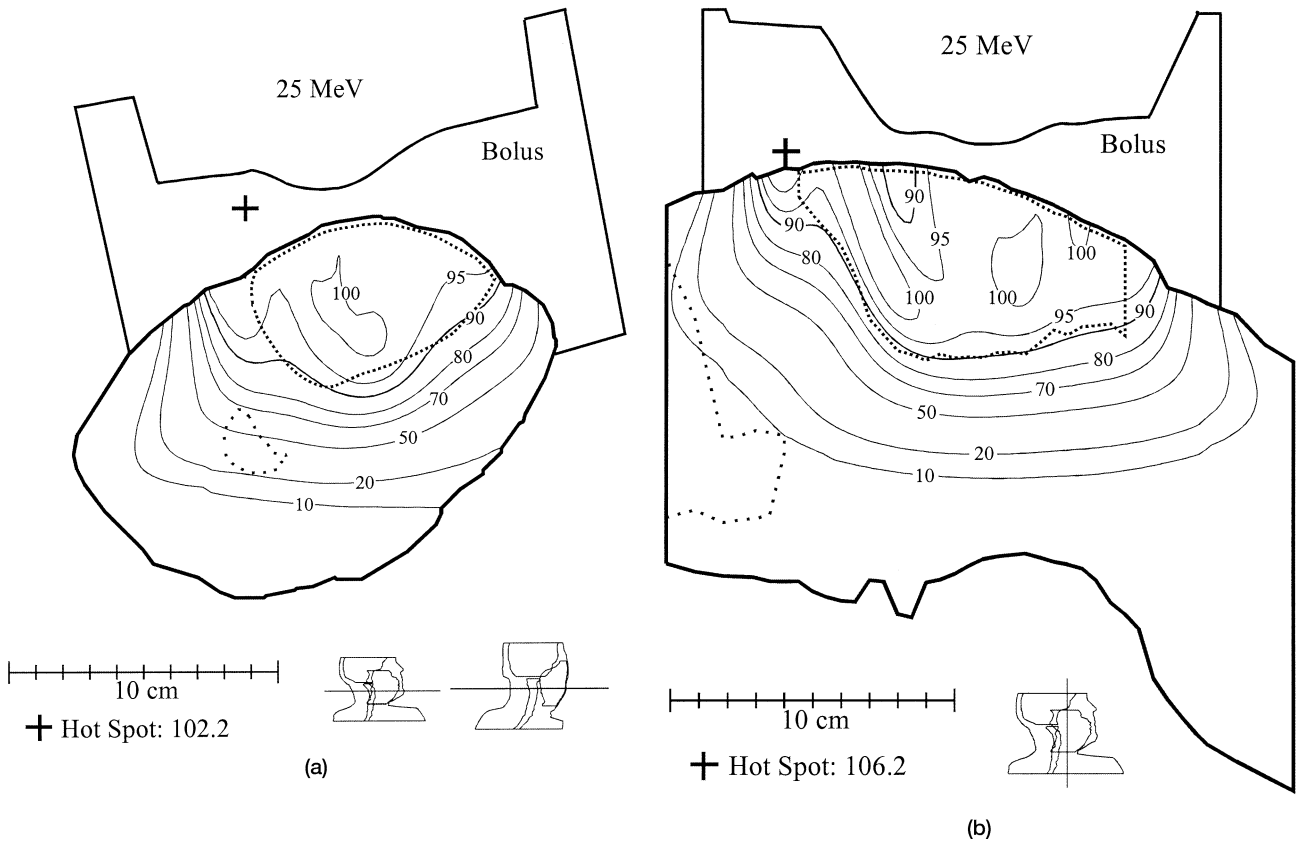
Fig. 13. Isodose distribution (%) for the head-and-neck, right buccal mucosa case, after intensity modulation. The treatment volume is delineated with the dashed contour (a) transverse slice, (b) coronal slice.
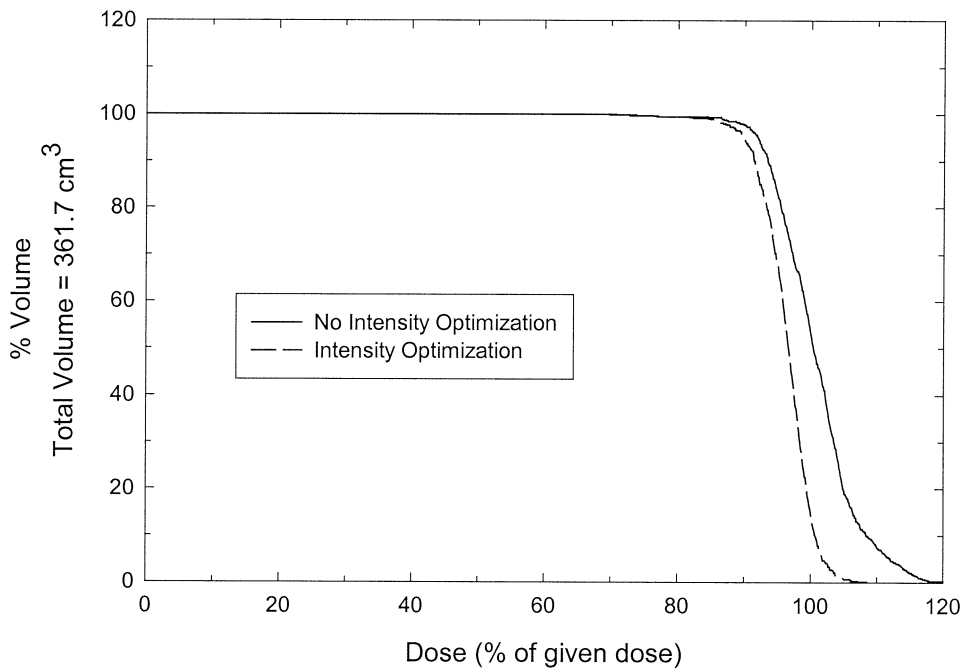

Fig. 14. Comparison of dose–volume histograms for the head-and-neck, right buccal mucosa case, before (solid line) and after (dashed line) intensity modulation.
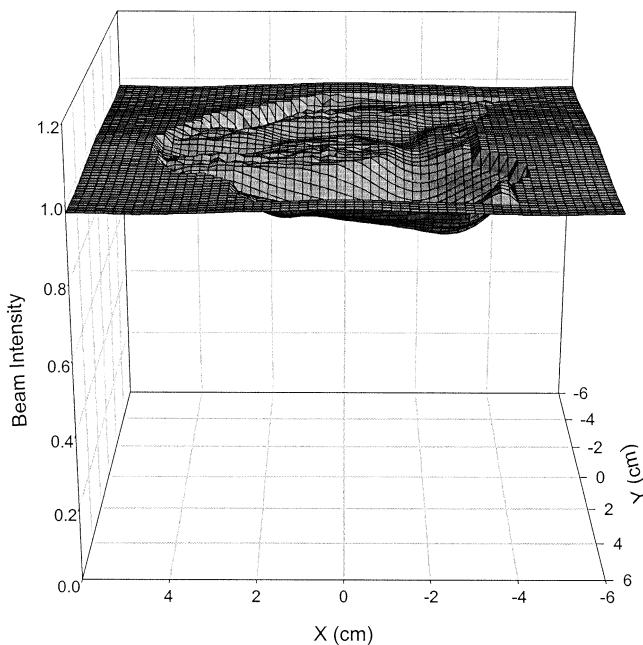
Fig. 15. Intensity profile after modulation for the head-and-neck, right buccal mucosa case.

that for the MM50 racetrack microtron, an MLC position of 67.5 cm and an SSD of 85 cm allows electron beam shaping that is similar to that with conventional electron beam shaping applicators at 90 cm and an SSD of 110 cm (21). Karlsson *et al.* have shown how modifications such as helium in the head, lowering the MLC position to 65 cm, and shortening the SSD can give acceptable penumbra width (22).

Another attractive alternative is an electron MLC, which has the benefit of allowing the patient's SSD to remain the same and to achieve similar penumbra width. Ma *et al.* have reported on attaching a prototype manual MLC to the bottom scraper of the electron applicator, which could also be used for electron intensity modulation (15). It must be noted

here that with the introduction of the photon or electron MLC for electron intensity modulation will increase dose calculation complexity. Electron scattering from leaf ends, leaf leakage, and bremsstrahlung production, considerably affects the delivered dose and are factors that must be taken into account in the computation of dose.

CONCLUSIONS

We have demonstrated that electron conformal therapy using bolus leads to volumes of increased or decreased dose (hot or cold spots) within the PTV, which could result in normal tissue complications or tumor regrowth. The combination of intensity modulation and bolus (energy modulation) improves dose homogeneity in the PTV while maintaining a high level of dose conformation to the PTV. This improvement showed greater benefit in the head-and-neck site than in the chest wall and thorax.

We expect intensity modulation to be achieved by the use of an MLC, either an X-ray or electron-specific MLC. The MLC leaves should be in the beam for only a short fraction of the total monitor units. Hence, intensity modulation along with the use of electron bolus should not significantly increase the monitor units and the corresponding treatment time.

Implementing this technology in the clinic will require the availability of treatment-planning systems that can design bolus and intensity modulation, technology that is demonstrated in the present work. It will also require access to computer-controlled milling machines or services that can mill the bolus, as well as access to MLCs capable of providing intensity modulation. Only MLC technology remains an area in need of further development. As that technology evolves, it will be important to model all of its functionality in the treatment-planning system. In the long term, it will be important to compare the dosimetric and clinical advantages and disadvantages of nonbolus electron conformal therapy techniques, which employ multiple intensity-modulated beams of differing energies, as have been presented by Åsell *et al.* (23) and Ebert and Hoban (24).

REFERENCES

1. Hogstrom KR. Conformal therapy with electron beams. In: Proceedings of the Varian 14th User's Meeting, Waikoloa, Hawaii; 1992. p. 45–48.
2. Khan FM, Doppke KP, Hogstrom KR, *et al.* Clinical electron-beam dosimetry: Report of AAPM Radiation Therapy Committee Task Group No. 25. *Med Phys* 1990;18:73–109.
3. Hogstrom KR, Steadham RS, Wong P, *et al.* Monitor unit calculations for electron beams. In: Gibbons JP, editor. Monitor unit calculations for external photon and electron beams. Madison, WI: Advanced Medical Physics Publishing; 2000. p. 113–126.
4. Hogstrom KR. Dosimetry of electron heterogeneities. In: Wright A, Boyer A, editors. Advances in radiation therapy treatment planning, AAPM Monograph #9. New York, NY: American Institute of Physics; 1983. p. 223–243.
5. Hogstrom KR. Treatment planning in electron-beam therapy. In: Vaeth JM, Meyer JL, editors. Frontiers in radiation therapy

oncology. Farmington, CT: Karger Publishing; 1991. p. 30–52.
6. Archambeau JO, Forell B, Doria R, *et al.* Use of variable thickness bolus to control electron beam penetration in chest wall irradiation. *Int J Radiat Oncol Biol Phys* 1981;7:835–842.
7. Beach JL, Coffey CW, Wade JS. Individualized chest wall compensating bolus for electron irradiation following mastectomy: An ultrasound approach. *Int J Radiat Oncol Biol Phys* 1981;7:1607–1611.
8. Low DA, Starkschall G, Bujnowski SW, *et al.* Electron bolus design for radiotherapy treatment planning: Bolus design algorithms. *Med Phys* 1992;19:115–124.
9. Starkschall G, Antolak JA, Hogstrom KR. Electron beam bolus for 3-D conformal radiation therapy. In: Purdy JA, Emami B, editors. 3-D radiation treatment planning and conformal therapy. Madison, WI: Medical Physics Publishing; 1993. p. 265–282.

10. Low DA, Starkschall D, Sherman NE, *et al.* Computer aided design and fabrication of an electron bolus for treatment of the paraspinal muscles. *Int J Radiat Oncol Biol Phys* 1995;33: 1127–1138.

11. Perkins GH, McNeese MD, Antolak JA, *et al.* A custom three dimensional electron bolus technique for optimization of post-mastectomy irradiation. *Int J Radiat Oncol Biol Phys* 2001; 51:1142–1151.

12. Bawiec ER. The effects of accuracy in milling of electron bolus on dose delivery. M.S. thesis, The University of Texas Graduate School of Biomedical Sciences, Houston, TX, 1994.

13. Purdy JA, Klein EE. External photon beam dosimetry and treatment planning. In: Perez CA, Brady LW, editors. Principles and practice of radiation oncology. 3rd ed. Philadelphia: Lippincott-Raven Publishers; 1997. p. 281–320.

14. Kudchadker RJ, Hogstrom KR, Boyd RA. Multileaf collimation for electron intensity modulation (Abstr.). *Med Phys* 2000;27:1375.

15. Ma CM, Pawlicki T, Lee MC, *et al.* Energy and intensity modulated electron beams for radiotherapy. *Phys Med Biol* 2000;45:2293–2311.

16. Hyödynmaa S, Gustafsson A, Brahme A. Optimization of conformal electron beam therapy using energy and fluence modulated beams. *Med Phys* 1996;23:659–666.

17. Hogstrom KR, Mills MD, Almond PR. Electron beam dose calculations. *Phys Med Biol* 1981;26:445–459.

18. Starkschall G, Shiu AS, Bujnowski SW, *et al.* Effect of dimensionality of heterogeneity corrections on the implementation of a three-dimensional electron pencil-beam algorithm. *Phys Med Biol* 1991;36:207–227.

19. Antolak JA, Hogstrom KR, Rosen I. Optimization of electron bolus design (Abstr.). *Med Phys* 1996;23:1101.

20. Klein EE, Li Z, Low DA. Feasibility study of multileaf collimated electrons with a scattering foil based accelerator. *Radiother Oncol* 1996;41:189–196.

21. Moran JM, Martel MK, Bruinvis IAD, *et al.* Characteristics of scattered electron beams shaped with a multileaf collimator. *Med Phys* 1997;24:1491–1498.

22. Karlsson MG, Karlsson M, Ma CM. Treatment head design for multileaf collimated high-energy electrons. *Med Phys* 1999;26:2161–2167.

23. Åsell M, Hyödynmaa S, Gustafsson A, *et al.* Optimization of 3D conformal electron beam therapy in inhomogeneous media by concomitant fluence and energy modulation. *Phys Med Biol* 1997;42:2083–2100.

24. Ebert MA, Hoban PW. Possibilities for tailoring dose distributions through the manipulation of electron beam characteristics. *Phys Med Biol* 1997;42:2065–2081.